DAOSTORM: an algorithm for high-density super-resolution microscopy

To the Editor: Astronomy and biology have more in common than you might expect. Here we show that methods originally used to study crowded stellar fields can improve the performance of localization-based super-resolution microscopies (stochastic optical reconstruction microscopy (STORM)[1], photoactivated localization microscopy[2] and others), which currently have slow imaging rates (typically < 0.01 image s^{-1}), limiting their utility in studies of live-cell dynamics.

These techniques, which use stochastic photoswitching to resolve closely spaced fluorophores and thus reconstruct super-resolved images, require that the specimen has a low density of active fluorophores (hereafter called 'imaging density'; <1 molecule μm^{-2}), limiting imaging speed and spatial resolution (**Supplementary Discussion**). A major cause of this issue is that current super-resolution localization algorithms work by fitting images of fluorescent molecules using only a single model point spread function (PSF; the diffraction-limited image of a fluorophore). We observed that astronomy software, DAOPHOT II (refs. 3,4), can simultaneously fit overlapping molecular PSFs (hereafter called 'molecules') with multiple model PSFs instead of just one, facilitating analysis at high imaging density (up to 10 molecules μm^{-2}). We developed DAOSTORM (**Supplementary Software** and **Supplementary Note**), which adapts DAOPHOT II for super-resolution imaging by increasing its automation and robustness (**Supplementary Fig. 1** and **Supplementary Methods**).

We compared DAOSTORM to two common localization algorithms. 'Sparse algorithm 1' (SA1)[1] fits candidate molecules with a single Gaussian PSF of variable size and ellipticity. Localizations arising from overlapping molecules are rejected if the fitted PSF appears too elliptical (shape-based filtering), too large or too small (size-based filtering). 'Sparse algorithm 2' (SA2)[5] fits candidate molecules with a single Gaussian PSF of fixed shape and size, without shape- or size-based filtering.

We first investigated the qualitative performance of each algorithm for images of Alexa Fluor 647–immunolabeled microtubules in fixed COS-7 cells. We recorded data at high imaging density using total internal reflection fluorescence microscopy and direct (d)STORM photoswitching conditions[5] (100 ms integration time, ~4,000 photons fluorophore^{-1} frame^{-1}). We plotted localizations on raw images, illustrating the characteristic performance of each algorithm (**Fig. 1a**). SA1 only localized isolated molecules, which were fitted with small localization error. SA2 localized a larger fraction of the molecules but yielded large localization errors for overlapping molecules. DAOSTORM outperformed both sparse algorithms, identifying almost all molecules with small localization error.

We quantified the performance of each algorithm by analyzing simulations of randomly distributed surface-immobilized fluorophores[6]. We compared observed localizations to simulated positions, calculating the recall[5] and localization error at different imaging densities. Recall is the percentage of simulated fluorophores detected. Localization error is the root-mean-square distance between a localization and the simulated position. We also measured the precision[5] and redundancy (**Supplementary Methods**), which did not vary substantially.

DAOSTORM substantially outperformed the sparse algorithms in simulations at high signal-to-noise ratio typical of STORM data (bright organic fluorophores, 5,000 photons molecule^{-1} frame^{-1}; **Fig. 1b-c**). SA1 showed poor recall at high density, with imaging density at half-maximum recall, ρ_{HM}, of 1.2 molecule μm^{-2}. However, SA1 yielded small localization errors even at high imaging density because most overlapping molecules were rejected. SA2 had better recall performance (ρ_{HM} = 3.4 molecules μm^{-2}) but gave large localization errors even at low imaging density (>0.1 molecules μm^{-2}). In contrast, DAOSTORM gave small localization errors similar to the other 'precise' algorithm, SA1, together with a sixfold improvement in recall performance (ρ_{HM} = 7.5 molecules μm^{-2}). For simulations at low signal-to-noise ratio typical of photoactivated localization microscopy data (fluorescent proteins, 200 photons molecule^{-1} frame^{-1};

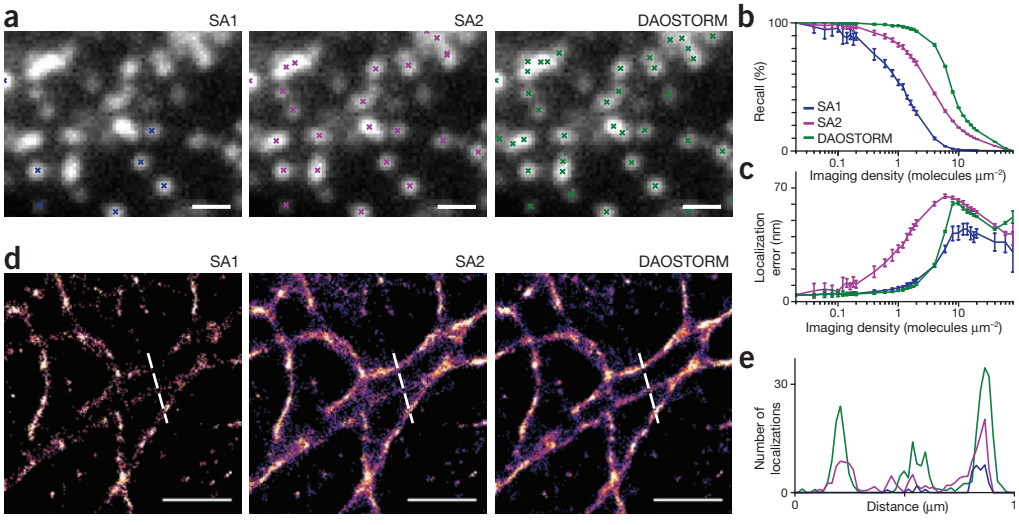

Figure 1 | Comparison of DAOSTORM to existing super-resolution localization algorithms. (**a**) A single image of fluorescently labeled microtubules was analyzed using SA1, SA2 and DAOSTORM. Crosses represent localizations for each algorithm (**b**,**c**) Recall (**b**) and localization error (**c**) of the algorithms used in **a** measured for simulated images of randomly distributed surface-immobilized molecules. Error bars, s.d. (n = 10). (**d**) Super-resolved microtubule images from a 2,000-frame data series. (**e**) Line plots of cross-section indicated by dashed lines in **d**. Scale bars, 1 μm.

Supplementary Fig. 2), DAOSTORM gave a twofold increase in ρ_{HM}.

Next, we recorded 2,000 dSTORM images of the microtubule network described above and used each algorithm to obtain super-resolved images (**Fig. 1d**). SA1 had low recall, producing poorly sampled STORM images, and SA2 achieved higher recall but with large localization error, leading to poorly defined, noisy images. DAOSTORM had high recall and small localization error, producing well-defined, low-noise images. A line plot across three parallel microtubules demonstrated the performance difference among the algorithms (**Fig. 1e**): DAOSTORM resolved all three microtubules, SA2 detected two and SA1 detected only one. We also compared additional line plots across the images and plotted the fluorescence average of the data (**Supplementary Figs. 3** and **4**).

These results demonstrated the ability of DAOSTORM to provide a more quantitative report of spatial distribution of fluorescent molecules, to increase quality of super-resolved images of biological samples and to maintain performance at high imaging density. Our algorithm will be useful for all localization-based super-resolution methods because it maximizes information content extracted from raw data and increases both imaging speed and maximum spatial resolution; these improvements will be particularly useful for challenging applications such as live-cell super-resolution imaging.

DAOSTORM currently uses a fixed-shape model PSF for fitting; an extension using PSFs with variable shape will allow fitting to fluorophores with fixed dipole orientation[7] and combination with three-dimensional STORM methods. DAOSTORM also has the potential to reduce data acquisition time in fields besides super-resolution microscopy, such as fluorescence imaging–based DNA sequencing[8].

Note: Supplementary information is available on the Nature Methods website.

ACKNOWLEDGMENTS

We thank K. Finan, S. Baboo and P.R. Cook (University of Oxford) for COS-7 cells, and S. van de Linde, U. Endesfelder, M. Heilemann and M.A. Little for technical assistance. S.J.H., S.U. and A.N.K. were supported by Biotechnology and Biological Sciences Research Council grant BB/H0179SX/1 and Bionanotechnology Interdisciplinary Research Collaboration grant GR/R45659/01. This research was funded by the EU Seventh Framework Programme (FP7/2007-2013; grant 201418, READNA). S.U. was supported by MathWorks, USA.

COMPETING FINANCIAL INTERESTS

The authors declare no competing financial interests.

Seamus J Holden, Stephan Uphoff & Achillefs N Kapanidis

Biological Physics Research Group, Clarendon Laboratory, Department of Physics, University of Oxford, Oxford UK.
e-mail: s.holden1@physics.ox.ac.uk or a.kapanidis1@physics.ox.ac.uk

1. Rust, M.J., Bates, M. & Zhuang, X. *Nat. Methods* **3**, 793–795 (2006).
2. Betzig, E. *et al. Science* **313**, 1642–1645 (2006).
3. Stetson, P.B. *Publ. Astron. Soc. Pacific* **99**, 191–222 (1987).
4. Agrawal, A., Deo, R., Wang, G.D., Wang, M.D. & Nie, S. *Proc. Natl. Acad. Sci. USA* **105**, 3298–3303 (2008).
5. Wolter, S. *et al. J. Microsc.* **237**, 12–22 (2010).
6. Holden, S.J. *et al. Biophys. J.* **99**, 3102–3111 (2010).
7. Mortensen, K.I., Churchman, L.S., Spudich, J.A. & Flyvbjerg, H. *Nat. Methods* **7**, 377–381 (2010).
8. Lipson, D. *et al. Nat. Biotechnol.* **27**, 652–658 (2009).